Available online at www.sciencedirect.com

SciVerse ScienceDirect

Procedia IUTAM 00 (2012) 000-000

Procedia IUTAM

www.elsevier.com/locate/procedia

Conference Title

High order Poisson solver for unbounded flows

Mads Mølholm Hejlesen[a], Johannes Tophøj Rasmussen[a], Philippe Chatelain[b], Jens Honoré Walther[a,c,*]

[a] *Department of Mechanical Engineering, Technical University of Denmark, Building 403, DK-2800 Kgs. Lyngby, Denmark*
[b] *Institute of Mechanics, Materials and Civil Engineering, Université catholique de Louvain, B-1348, Belgium*
[c] *Computational Science and Engineering Laboratory, ETH Zürich, Universitätsstrasse 6, CH-8092 Zürich, Switzerland*

Abstract

We present a high order method for solving the unbounded Poisson equation on a regular mesh using a Green's function solution. The high order convergence is achieved by formulating mollified integration kernels, derived from a filter regularisation of the solution field. The method is implemented on a rectangular domain using fast Fourier transforms (FFT) to increase computational efficiency. We extend the Poisson solver to directly solve the derivatives of the solution. This is achieved either by including the differential operator in the integration kernel or by performing the differentiation as a multiplication of the Fourier coefficients. In this way differential operators such as the divergence or curl of the solution field can be solved to the same high order convergence without additional computational effort. The method is applied and validated, however not restricted, to the equations of fluid mechanics, and can be used in many physical problems to solve the Poisson equation on a rectangular unbounded domain. For the two-dimensional case we propose an infinitely smooth test function which allows for arbitrary high order convergence. Using Gaussian smoothing as regularisation we document an increased convergence rate up to tenth order. The method however, can easily be extended well beyond the tenth order. To show the full extend of the method we present the special case of a spectrally ideal regularisation of the velocity formulated integration kernel, which achieves an optimal rate of convergence.

Keywords: Type your keywords here, separated by semicolons ;

1. Introduction

In particle based vortex methods the Poisson equation arises when calculating the stream function or velocity field from the vorticity. This is usually solved by applying a Green's function solution in form of the Biot-Savart equation [1]. Here each particle induce a velocity onto every other particle in the system and thus poses an N_p-body problem. The direct evaluation of the mutual particle interaction amounts to an inefficient scaling of $\mathcal{O}(N_p^2)$ and alternative methods have been developed in order to obtain a more efficient scaling.

One solution to the scaling problem is found in tree algorithms such as the Barnes-Hut [2] or the fast multipole method (FMM) [3]. Here the particles are grouped according to particle density and distance to the evaluated particle

* Corresponding author. Tel.: + 45 4525 4327; fax: + 45 4588 4325.
E-mail address: jhw@mek.dtu.dk

and only the collective contribution from the group is considered. The FMM does not rely on any mesh and is capable of achieving an optimal scaling of $\mathcal{O}(N_p)$, however, it is subject to a large pre-factor when constructing and traversing the tree data structure.

Another, inconvenience of mesh-free vortex methods is the lack of a provable convergence theory. This has motivated development of particle remeshing [4, 5] and hybrid particle-mesh methods such as the vortex-in-cell (VIC) method by Christiansen [6]. The VIC method solves the Poisson equation by interpolating the particle vorticity to a regular mesh where the velocity is calculated by a mesh based solver. This ensures the numerical convergence of the method and enables efficient mesh based Poisson solvers and finite difference stencils for evaluation of derivatives.

The Poisson solver of Hockney and Eastwood [7] utilises the regular mesh of the VIC method through highly efficient fast Fourier transforms (FFT). The method is based on calculating a Green's function solution through the convolution of the vorticity field with the Green's function. This is effectively performed by Fourier transforming the vorticity field and integration kernel whereas the convolution is done by a simple multiplication of the discrete Fourier coefficients. In a periodic domain, spectral differentiating is obtained in Fourier space simply by multiplying the coefficients with their respective wavenumber. Furthermore, the periodic boundary condition is naturally treated by the periodicity of the Fourier series and a spectral convergence is therefore easily obtained as shown by Rasmussen [8]. For the unbounded free-space problem, the integration kernel can not be represented exactly in Fourier space due to the inherent periodicity of the Fourier transform. On the same ground the domain must be extended to twice the size, to avoid the periodicity of the discrete convolution.

Hockney and Eastwood [7] showed that it is possible to impose free-space boundary conditions by zero-padding the vorticity field and convolving this with a free-space integration kernel of equal size. At first sight, extending the domain size to $2N$ in each unbounded direction increases the computational scaling of the d-dimensional solver to $\mathcal{O}(2^d dN^d \log(2N))$ and requires an allocated memory of $(2N)^d$ for a fully unbounded domain. However, an FFT based convolution algorithm, proposed by [7], significantly reduces the computational scaling and the memory needed. This is done by exploiting the fact that a multidimensional Fourier transform consists of series of one-dimensional transforms carried out in each direction, sequentially. The method of Hockney and Eastwood can be extended to mixed periodic-free boundary conditions as shown by Chatelain and Koumoutsakos [9].

In the present work the Green's function based Poisson solver is extended to achieve a high order of convergence of the convolution integral for a continuous field by formulating regularised integration kernels. These are derived based on the work of [10, 11, 12, 13, 14] who used smoothing functions to achieve high order regularised integration kernels for mesh-free vortex methods. However, unlike mesh-free methods, the mesh-based Poisson solver requires a non-singular, continuous integration kernel to ensure an accurate numerical solution. Therefore, a great effort is put into defining the centre value of the regularised integration kernels as this is identified as a crucial factor for achieving high order convergence [8].

In this paper we will show the derivation and validation of a high order Poisson solver in the two-dimensional case ($d = 2$). For this we introduce mollified integration kernels, similarly to [10, 11, 12, 13, 14], which is derived by regularisation of the vorticity field. In this work we choose Gaussian smoothing as regularisation and achieve an increased order by defiltering the smoothing filter to conserve higher order moments of the vorticity field. Furthermore, a special case is presented where a velocity kernel is derived using a spectrally ideal regularisation by which an optimal convergence rate is achieved. The solver is extended to directly calculate the velocity field to an equally high order as the Poisson solver without any additional numerical effort. For the three-dimensional case, which is similar in both derivation and results, the reader is referred to [15].

2. The Poisson equation in fluid mechanics and its Green's function solution

In fluid kinematics, the vorticity, ω is defined as the curl of the velocity $u = (u, v)$

$$\omega \equiv \nabla \times u. \tag{1}$$

This can be inverted to find the velocity by defining a solenoidal vector potential (ψ: $\nabla \cdot \psi = 0$) referred to as the stream function

$$u \equiv \nabla \times \psi \tag{2}$$

This leads to Poisson equations for the stream function

$$\nabla^2 \psi = -\omega \tag{3}$$

and the velocity field

$$\nabla^2 u = -\nabla \times \omega. \tag{4}$$

Using a Green's function approach, the Poisson equation (Eq. (3)) can be solved on the unbounded domain $\mathbb{R}^d$ through the convolutions

$$\psi(x) = \int_{\mathbb{R}^d} G(x-\xi)\omega(\xi)\, d\xi = G * \omega \tag{5}$$

or for the velocity (Eq. (4))

$$u(x) = \int_{\mathbb{R}^d} K(x-\xi)\omega(\xi)\, d\xi = K * \omega \tag{6}$$

where $*$ denotes the discrete convolution operator. This relation is also shown by convolving the Poisson equation with a integration kernel G

$$\nabla^2 \psi = -\omega \quad \rightarrow \quad G * \nabla^2 \psi = -G * \omega \quad \rightarrow \quad -\psi * \nabla^2 G = G * \omega. \tag{7}$$

Thus by deriving the convolution kernel from

$$\nabla^2 G(x) = -\delta(x-\xi) \tag{8}$$

which is also known as the Green's equation, where $\delta(x-\xi)$ is the Dirac delta function, we obtain

$$\psi = G * \omega \tag{9}$$

The integration kernel for the two-dimensional case derived from Eq. (8) is the well known Green's function for the two-dimensional free-space Poisson equation

$$G(x) = -\frac{1}{2\pi} \log|x| \qquad \text{for } \mathbb{R}^2. \tag{10}$$

The corresponding velocity representation is

$$u = K * \omega \tag{11}$$

where $K(x) = \nabla G(x) \times$ is given by

$$K(x) = -\frac{1}{2\pi|x|^2} \begin{pmatrix} y \\ -x \end{pmatrix} \qquad \text{for } \mathbb{R}^2. \tag{12}$$

The integration kernels of Eqs. (10) and (12) are both singular at $|x| = 0$ and results in an $\mathcal{O}(h^2)$ convergence of the Poisson solver where h is the discretisation length.

3. Unbounded Poisson solver based on fast Fourier transforms

The convolutions of Eqs. (9) and (11) can be solved for free-space boundary conditions by performing the discrete convolution in a linear sense. This is done by zero-padding the vorticity field to twice the domain size and convolving the now zero-padded vorticity field and the fully defined integration kernel of equal size. The convolution is performed efficiently in Fourier space whereas the linearity of the problem also enables differentiation and thereby curl of Eq. (4) to be carried out in Fourier space, thus reducing the number of integration kernels needed. The convolution equations in Fourier space are written as

$$\widehat{\psi} = \widehat{G}\,\widehat{\omega} \qquad \text{and} \qquad \widehat{u} = \widehat{K}\,\widehat{\omega} \qquad \text{or} \qquad \widehat{u} = \imath k \times \widehat{\psi} \tag{13}$$

where $\hat{\cdot}$ denotes the Fourier coefficients obtained by discrete Fourier transforms, $\imath$ is the imaginary unit and $k = \{k_x, k_y(, k_z)\}$ is the wavenumber corresponding to the respective Fourier coefficient. In 2D we only solve the out-of-plane component as $w = \{0, 0, \omega_3\}$ and $\psi = \{0, 0, \psi_3\}$ hence the rank of K in Eq. (12).

The domain doubling technique has a severe impact on the convolution footprint, however it can be reduced from $(2N)^d$ to $2N^d + (2N)^{d-1}$. Hockney and Eastwood [7] propose to carry out a transform in one direction and then proceed row by row for $d = 2$ or plane by plane for $d = 3$. Here the remaining dimension(s) is zero-padded, Fourier-transformed, multiplied by $\hat{G}$ and inverse transformed whereas the zero-padding is truncated before moving on to next row or plane. This method, however, still requires the integration kernels G or K to be calculated initially and stored in their full size of $(2N)^d$.

4. Derivation of regularised integration kernels

We now look into the construction of the integration kernels and how to derive high order integration kernels by regularising the given scalar or vector field. In the present work, we achieve higher order by using a regularised particle representation [10, 11, 12, 13, 14]. Effectively, a regularisation of the vorticity field is considered

$$\omega_\zeta = \zeta * \omega \tag{14}$$

where ζ is a conserving filter. The convolution of the filter kernel with the Green's function can be written as

$$\psi = G * (\zeta * \omega) = (G * \zeta) * \omega = G_\zeta * \omega. \tag{15}$$

For a given filter function ζ, the corresponding integration kernel G_ζ can be derived. For simplicity this is performed in polar (r, θ) coordinates for $\mathbb{R}^2$. The regularised Green's equation analogous to Eq. (8) is given by

$$-\zeta(r) = \nabla^2 G_\zeta(r) = \frac{1}{r}\frac{d}{dr}\left(r\frac{dG_\zeta}{dr}\right) \tag{16}$$

where ε is a filter normalisation factor. The weight function w is defined from the filter function as

$$w(r) = \int_0^r \zeta(t)\,\mathrm{d}t = 2\pi\int_0^r t\zeta(t)\,\mathrm{d}t. \tag{17}$$

Combining Eqs. (16) and (17) renders an expression for the regularised integration kernel

$$G_\zeta(r) = -\frac{1}{2\pi}\int \frac{w(r)}{r}\,\mathrm{d}r \tag{18}$$

5. High order smoothing functions and corresponding integration kernels

From Eq. (16) it is seen that for the derivation of higher order integration kernels the Green's equation is substituted by a regularised version

$$\nabla^2 G(r) = -\delta(r) \qquad \rightarrow \qquad \nabla^2 G_\zeta(r) = -\zeta(r) \tag{19}$$

and thus ζ represents some approximation to the delta function. Its conservation properties can be determined by its frequency response given by the Fourier transform. For this we introduce the radial Fourier transforms, where $k = 1/r$ is the radial wavenumber

$$\hat{\zeta}(k) = (2\pi)^{\frac{d}{2}}\int_0^\infty \zeta(r)\frac{J_{\frac{d}{2}-1}(kr)}{(kr)^{\frac{d}{2}-1}}r^{d-1}\,\mathrm{d}r \qquad \text{and} \qquad \zeta(r) = \frac{1}{(2\pi)^{\frac{d}{2}}}\int_0^\infty \zeta(k)\frac{J_{\frac{d}{2}-1}(kr)}{(kr)^{\frac{d}{2}-1}}k^{d-1}\,\mathrm{d}k \tag{20}$$

Here J_ν is the Bessel function of order ν.

The filter function may be described from a number of different filters, which as a minimum must have conservative properties i.e. $\int_{\mathbb{R}^d}\zeta(x)\,dx = 1$ or equally $\hat{\zeta}(0) = 1$. In this work we present the derivation and convergence of a class of high order Gaussian filters and show the special case of an ideal filter based on Bessel functions.

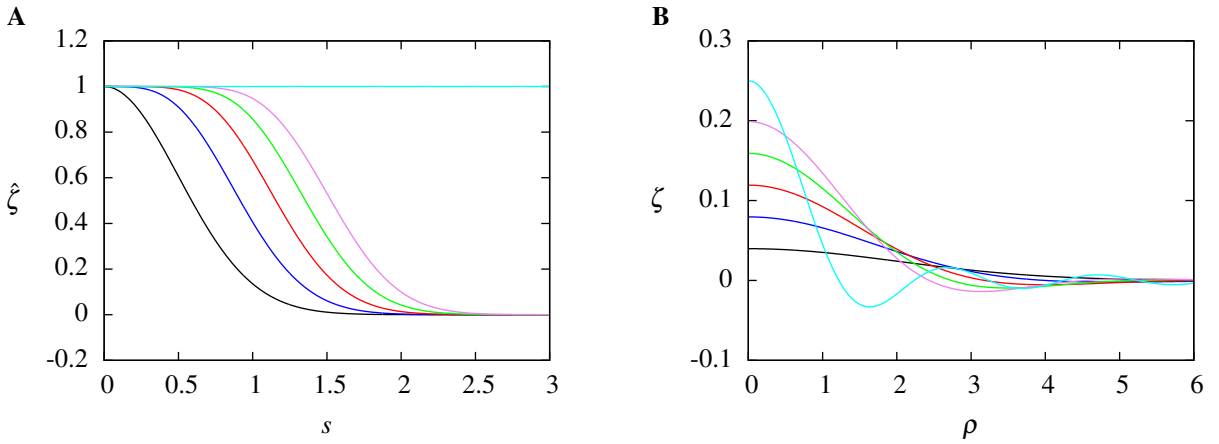

Fig. 1. The frequency response of the regularisation filter (A) and the corresponding filter functions in real space (B). The Gaussian smoothing functions ζ_g with $\varepsilon = 2h$ for $m = 2$: (——); $m = 4$: (——); $m = 6$: (——); $m = 8$: (——); $m = 10$: (——), and the Bessel function regularisation ζ_J (——).

5.1. Regularisation by Gaussian smoothing

One type of regularisation is obtained by Gaussian smoothing of the vorticity field. For this, the regularisation filter is given by the Gaussian smoothing function ζ_g which, along with its frequency response $\hat{\zeta}_g$, is given by

$$\zeta_g(r) = \frac{1}{(2\pi\varepsilon^2)^{d/2}} \exp\left(-\frac{\rho^2}{2}\right) \qquad \text{and} \qquad \hat{\zeta}_g(k) = \exp\left(-\frac{s^2}{2}\right). \tag{21}$$

Here $\rho = r/\varepsilon$ and $s = k\varepsilon$ are the radial coordinate and wavenumber normalised with ε, which in this case represents a smoothing radius. The frequency response has a bandwidth of $\sqrt{2}$ and gives a second order smoothing. A higher order smoothing is obtained by increasing the bandwidth of the frequency response thus increasing the conservation properties of the filter, as seen in Fig. 1.

A high order Gauss filter ζ_m of order m can be obtained by the defiltering

$$\hat{\zeta}_m = D_m \hat{\zeta}_g \tag{22}$$

where D_m is an approximation of the inverse filter response. To find D_m we use the Taylor expansion of the inverse Gauss filter which is given by

$$\left(\exp\left(-\frac{s^2}{2}\right)\right)^{-1} = 1 + \frac{1}{2}s^2 + \frac{1}{8}s^4 + \frac{1}{48}s^6 + \ldots = \sum_{n=0}^{\infty} \frac{(s^2/2)^n}{n!}. \tag{23}$$

An m-th order Taylor expansion is then obtained by the truncated series

$$D_m = \sum_{n=0}^{m/2-1} \frac{(s^2/2)^n}{n!}. \tag{24}$$

Thus the frequency response of an m-th order Gaussian filter is given by

$$\hat{\zeta}_m(k) = \sum_{n=0}^{m/2-1} \frac{(s^2/2)^n}{n!} \exp\left(-\frac{s^2}{2}\right). \tag{25}$$

Using the inverse Fourier transform of Eq. (20) the smoothing functions are obtained. The 2D smoothing functions for $m = 4, 6, 8, 10$ are given by

$$\zeta_4(r) = \left(2 - \frac{1}{2}\frac{r^2}{\varepsilon^2}\right)\frac{\exp\left(-\frac{r^2}{2\varepsilon^2}\right)}{2\pi\varepsilon^2} \qquad \zeta_8(r) = \left(4 - 3\frac{r^2}{\varepsilon^2} + \frac{1}{2}\frac{r^4}{\varepsilon^4} - \frac{1}{48}\frac{r^6}{\varepsilon^6}\right)\frac{\exp\left(-\frac{r^2}{2\varepsilon^2}\right)}{2\pi\varepsilon^2}$$
$$\zeta_6(r) = \left(3 - \frac{3}{2}\frac{r^2}{\varepsilon^2} + \frac{1}{8}\frac{r^4}{\varepsilon^4}\right)\frac{\exp\left(-\frac{r^2}{2\varepsilon^2}\right)}{2\pi\varepsilon^2} \quad \zeta_{10}(r) = \left(5 - 5\frac{r^2}{\varepsilon^2} + \frac{5}{4}\frac{r^4}{\varepsilon^4} - \frac{5}{48}\frac{r^6}{\varepsilon^6} + \frac{1}{384}\frac{r^8}{\varepsilon^8}\right)\frac{\exp\left(-\frac{r^2}{2\varepsilon^2}\right)}{2\pi\varepsilon^2}. \quad (26)$$

The smoothing functions and their frequency response is shown in Fig. 1 for $\varepsilon = 2h$. It is seen that by increasing the order of the filter the bandwidth of the frequency response increases. This manifests in real-space as oscillations of the filter function and the conservation of higher order moments given by

$$0^\beta = 2\pi \int_0^\infty \rho^\beta \zeta_m(\rho)\rho \, d\rho \quad (27)$$

where $\beta = \{0, 2, ..., m-2\}$.

Once defined, the smoothing functions can be used to derive the integration kernel by Eqs. (17) and (18). The regularised integration kernels from m-th order Gaussian smoothing can be written on the general form

$$G_m(x) = -\frac{1}{2\pi}\left(\log(|x|) - R_m\left(\frac{|x|}{\varepsilon}\right)\exp\left(\frac{-|x|^2}{2\varepsilon^2}\right) + \frac{1}{2}\mathrm{E}_1\left(\frac{|x|^2}{2\varepsilon^2}\right)\right) \quad (28)$$

where R_m is an even polynomial which for $m = 4, 6, 8, 10$ gives

$$R_4(\rho) = \frac{1}{2} \qquad R_8(\rho) = \frac{11}{12} - \frac{7}{24}\rho^2 + \frac{1}{48}\rho^4$$
$$R_6(\rho) = \frac{3}{4} - \frac{1}{8}\rho^2 \qquad R_{10}(\rho) = \frac{25}{24} - \frac{23}{48}\rho^2 + \frac{13}{192}\rho^4 - \frac{1}{384}\rho^6. \quad (29)$$

In order to define $G_m(0)$ the exponential integral function $\mathrm{E}_1(z)$ can be expanded to an infinite series [16] by

$$\mathrm{E}_1(z) = -\gamma - \log(z) - \sum_{n=1}^{\infty}\frac{(-1)^n z^n}{n\,n!}. \quad (30)$$

The centre value $G_m(0)$ is then given by

$$G_m(0) = \lim_{x\to 0}(G_m) = \frac{1}{2\pi}\left(\frac{\gamma}{2} - \log\left(\sqrt{2}\varepsilon\right) + R_m(0)\right) \quad (31)$$

where $\gamma = 0.5772156649$ is Eulers constant. The corresponding velocity kernels, obtained by $K_m = \nabla G_m \times$, is on the general form

$$K_m(x) = -\frac{1}{2\pi|x|^2}\begin{pmatrix} y \\ -x \end{pmatrix}\left(1 - Q_m\left(\frac{|x|}{\varepsilon}\right)\exp\left(\frac{-|x|^2}{2\varepsilon^2}\right)\right) \quad (32)$$

where Q_m is an even polynomial which for $m = 2, 4, 6, 8$ gives

$$Q_4(\rho) = 1 - \frac{1}{2}\rho^2 \qquad Q_8(\rho) = 1 - \frac{3}{2}\rho^2 + \frac{3}{8}\rho^4 - \frac{1}{48}\rho^6$$
$$Q_6(\rho) = 1 - \rho^2 + \frac{1}{8}\rho^4 \qquad Q_{10}(\rho) = 1 - 2\rho^2 + \frac{3}{4}\rho^4 - \frac{1}{12}\rho^6 + \frac{1}{384}\rho^8. \quad (33)$$

The centre value of the velocity kernel is defined as $K_m(0) = 0$.

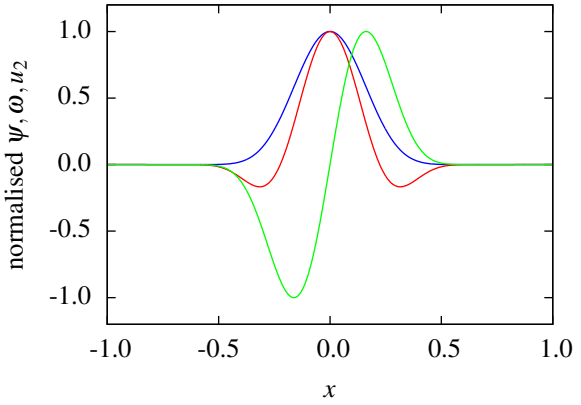

Fig. 2. The normalised test function and the corresponding solution for $c = 20$ and $R = 1$ at $(x,y) = (\cdot, 0)$. (——): Vorticity $\omega/\max(\omega)$; (——): Stream function $\psi/\max(\psi)$; (——): Velocity $v/\max(u)$.

5.2. Ideal regularisation by Bessel functions

As we wish to conserve the moments of the non-filtered field, an ideal regularisation filter is obtained when $\hat{\zeta}(s) = 1$ i.e. when every Fourier coefficient is conserved. For the 2D case it is seen from the radial Fourier transform (Eq. (20)) that an ideal filter regularisation can be obtained by the Bessel function

$$\zeta_J(r) = \frac{J_1(\rho)}{2\pi r} \tag{34}$$

whereas we obtain the frequency response

$$\hat{\zeta}_J(k) = 2\pi \int_0^\infty \zeta_J(r) J_0(kr) r \, \mathrm{d}r = \int_0^\infty J_1(r/\varepsilon) J_0(kr) \, \mathrm{d}r = 1. \tag{35}$$

Here the filter parameter ε determines the frequency of the Bessel function oscillations and not a smoothing radius as with the Gaussian smoothing. The oscillation of Bessel functions J_ν converges to a length of 2π. This means that the filter parameter is restricted by $\varepsilon \geq h/\pi$ and the optimal rate of convergence is found when $\varepsilon = h/\pi$.

From Eqs. (17) and (18) we get the corresponding integration kernel

$$G_J(r) = -\frac{1}{2\pi} \int \frac{1 - J_0(\rho)}{r} \, d\rho \tag{36}$$

which by the radial differentiation and Cartesian curl yields the velocity kernel

$$K_J(x) = -\frac{1 - J_0(\rho)}{2\pi |x|^2} \begin{pmatrix} y \\ -x \end{pmatrix} \tag{37}$$

6. Validation: compact vortex blob

To investigate the convergence of the free-space Poisson solver the test function i.e. the vorticity distribution, must be compact within the computational domain. This is achieved in the two-dimensional case by using a vortex blob to form a vorticity patch. In this study, we propose the use of a bump function distribution with an infinite number of continuous derivatives to avoid limitations of the convergence rate. The bump function is defined as

$$f(z) = \begin{cases} \exp\left(-\dfrac{c}{1-z^2}\right) & \text{for } |z| < 1 \\ 0 & \text{for } |z| \geq 1 \end{cases} \tag{38}$$

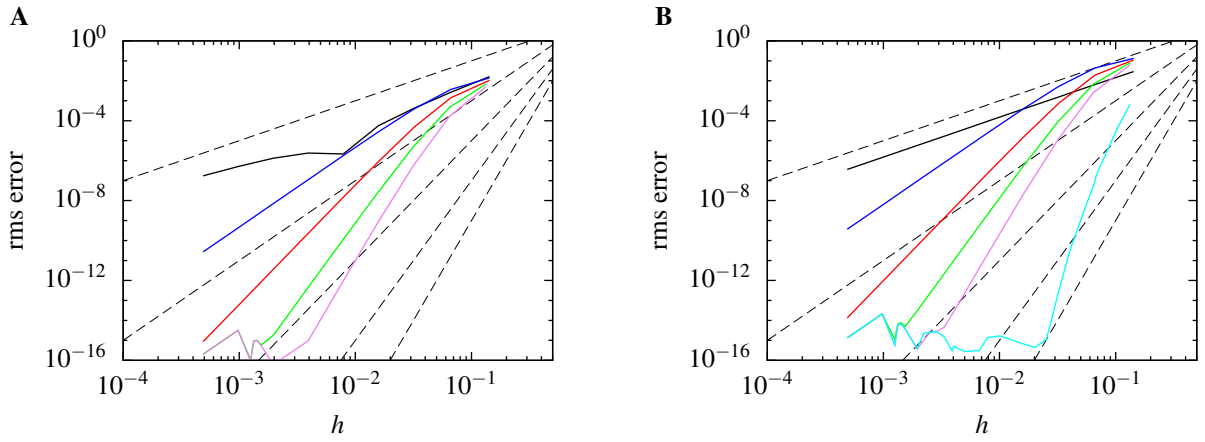

Fig. 3. The rms error of the resulting stream function (A) and velocity field (B) using Gaussian regularised integration kernels G_m and K_m with $\varepsilon = 2h$ and the ideal velocity kernel K_J. The calculated error for the velocity in (B) is virtually identical when calculated by the velocity kernels K_m as when using the integration kernel G_m with spectral differentiating in Eq. (13). (– – – –): from top h^2, h^4, h^6, h^8, h^{10}; (- - - -): round off error; (———): non-regularised kernels G and K; (———): $m = 4$; (———): $m = 6$; (———): $m = 8$; (———): $m = 10$; (———): K_J.

where c is an arbitrary positive constant set to 20 in this study. Using centred polar (r, θ) coordinates, the stream function is defined as

$$\psi = f\left(\frac{r}{R}\right) \tag{39}$$

where R is the radius of the vorticity patch. The initial vorticity field and the resulting velocity field are found analytically by Eq. (3) and Eq. (2), respectively, and is shown in Fig. 2.

The root-mean-squared (rms) error of the test case is shown in Fig. 3 for the regularised integration kernels G_m and K_m with $m = 4, 6, 8$ and K_J. As seen, the convergence rate of the Gaussian smoothed integration kernels corresponds to the respective design of the smoothing functions and the ideal velocity kernel K_J exhibits a spectral convergence. The same convergence rate is observed with the maximum error (not shown). The solution of the velocity field for the Gaussian based kernels are found to be practically identical, when using the velocity kernels K_m as when using the spectral differentiating in Eq. (13). Therefore, as spectral differentiating only uses a single integration kernel, it is considered the optimal choice in order to reduce the memory which is allocated for the integration kernels.

Evidently, it is only possible to reach a high convergence where the test function is sufficiently differentiable and resolved by the smoothing radius. However, during this study it was observed that a even though the convergence rate is restricted by the differentiability of the test function a lower error is still obtained when using a higher order integration kernel (not shown).

7. Investigations of the Gaussian smoothing radius

The application of a smoothing filter causes a smoothing error which is governed by the order of the filter [17, 18, 19, 20] and is is bounded by

$$\|\omega_\zeta - \omega\| < C_1\,\varepsilon^m\,\|\omega\|, \qquad \|\psi_\zeta - \psi\| < C_2\,\varepsilon^m\,\|\omega\| \qquad \text{and} \qquad \|u_\zeta - u\| < C_3\,\varepsilon^m\,\|\omega\| \tag{40}$$

where m is the order of the filter function.

Note that the discretisation of the convolution above leads to a second error contribution. It is due to the underlying quadrature of the integral at the grid points leading to a discretisation error of

$$\|\psi_\zeta - \psi_\zeta^h\| < C_4\,\varepsilon\left(\frac{h}{\varepsilon}\right)^l\|\omega\| \qquad \text{and} \qquad \|u_\zeta - u_\zeta^h\| < C_5\,\varepsilon^2\left(\frac{h}{\varepsilon}\right)^l\|\omega\|\,. \tag{41}$$

where l depends on the smoothness of the smoothing function ζ. As seen, the discretisation errors (Eqs. (41)), only converges when $\varepsilon > h$. This means that the particle kernel must overlap other particle locations which is a well-known behaviour in particle methods [17, 18, 19, 20, 21].

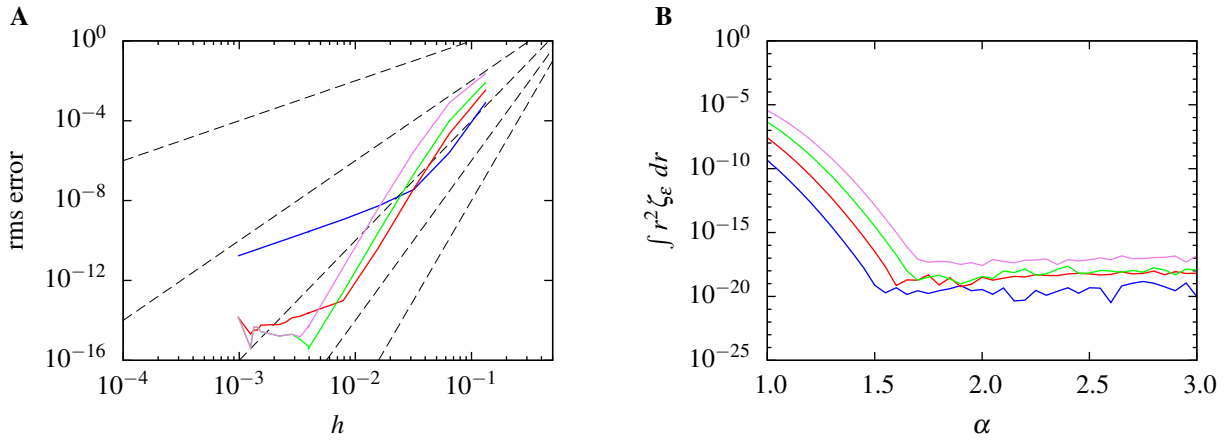

Fig. 4. (A) The rms error of the G_m integration kernel with $m = 10$ for $\varepsilon = \alpha h$ using different values of α. (– – – –): from top h^2, h^4, h^6, h^8, h^{10}; (——): $\alpha = 1.0$; (——): $\alpha = 1.25$; (——): $\alpha = 1.5$; (——): $\alpha = 1.75$. (B) The calculated discrete 2nd order moments of the Gaussian smoothing function ζ_m using different order kernels. (——): $m = 4$. (——): $m = 8$; (——): $m = 12$; (——): $m = 16$.

In the previous section, our validation relied on simply keeping $\varepsilon = \alpha h$ where $\alpha = 2$, was chosen. A more rigorous approach, which is consistent with the error behavior of the convolution, was suggested by Beale and Majda [20, 19, 12] in their convergence proof. They choose the smoothing radius as $\varepsilon = h^q$ with $0 < q < 1$. The corresponding error then scales as $\mathcal{O}(h^{qm})$, which can be made close to $\mathcal{O}(h^m)$ for q close to 1.

However, choosing the smoothing radius ε is not trivial as a too conservative choice of α might lead to a breakdown off the convergence rate, as seen in Fig. 4A, for the two-dimensional G_m kernel where $m = 10$. The same behaviour is also found using $\varepsilon = h^q$ when q is close to 1 (not shown). It is seen that keeping ε proportional to h will produce a $\mathcal{O}(h^{10})$ error, up to a certain point though. Eventually, the discretisation error overwhelms the smoothing error which causes the convergence rate to break down. This crossover point can be offset by increasing the overlap α, albeit at the cost of a higher smoothing error as seen in Fig. 4A.

In Fig. 4B it is seen to what extent the second discrete moment is conserved when using different values of α. We consider the Gaussian smoothing functions of $m = 4, 8, 12, 16$. It clearly shows that in order for the discrete moments to be satisfied to the accuracy of the quadrature i.e. at the kinks of the curves, the smoothing radius must be greater than the grid size by a margin or overlap α which is related to the order of the smoothing function m. We also observe that a higher order kernel will require a larger overlap to achieve the same moment error as a lower order one: as expected, higher order polynomials (Eq. (26)) require more points to be captured accurately.

8. Conclusion

A convolution integral method was presented for calculating the solution to the Poisson equation of a continuous field in an unbounded domain to an arbitrary high order of convergence. The regularisation method applied in mesh-free vortex methods to produce vortex blobs was combined with the FFT-based Poisson solver of particle-mesh methods to achieve a high rate of convergence without additional computational cost.

The method was shown to be able to calculate the derivative of the solution explicitly, either by direct spectral differentiating or by analytically differentiating the integration kernel. This enabled the evaluation of the curl to be performed directly by the solver and eliminates the need for an additional numerical scheme while maintaining the specified order of convergence. The two methods of calculating the derivative was found to give practically identical results and convergence behaviour. Thus as spectral differentiating only requires a single integration kernel, the allocated memory can be reduced by choosing this method.

Acknowledgements

The research has been supported by the Danish Research Council of Independent Research (Grant. No. 274-08-0258). We would also like to acknowledge the helpful discussions with Thomas Beale, Grégoire S. Winckelmans, Diego Rossinelli, Wim van Rees and Petros Koumoutsakos.

References

[1] Leonard A. Vortex Methods for Flow Simulation. J Comput Phys. 1980;37:289–335.

[2] Barnes J, Hut P. A hierarchical $O(N \log N)$ force-calculation algorithm. Nature. 1986;324(4):446–449.

[3] Carrier J, Greengard L, Rokhlin V. A fast adaptive multipole algorithm for particle simulations. SIAM J Sci Stat Comput. 1988;9(4):669–686.

[4] Koumoutsakos P, Leonard A. High-resolution simulation of the flow around an impulsively started cylinder using vortex methods. J Fluid Mech. 1995;296:1–38.

[5] Koumoutsakos P. Multiscale Flow Simulations Using Particles. Annu Rev Fluid Mech. 2005;37:457–487.

[6] Christiansen JP. Numerical Simulation of Hydrodynamics by the Method of Point Vortices. J Comput Phys. 1973;13:363–379.

[7] Hockney RW, Eastwood JW. Computer Simulation Using Particles. 2nd ed. Institute of Physics Publishing, Bristol, PA, USA; 1988.

[8] Rasmussen JT. Particle Methods in Bluff Body Aerodynamics [Ph.D. thesis]. Technical University of Denmark; 2011.

[9] Chatelain P, Koumoutsakos P. A Fourier-based elliptic solver for vortical flows with periodic and unbounded directions. J Comput Phys. 2010;229:2425–2431.

[10] Leonard A. Vortex Methods for Flow Simulation. J Comput Phys. 1980;37:289–335.

[11] Perlman M. On the accuracy of vortex methods. J Comput Phys. 1985;59:200–223.

[12] Beale JT, Majda A. High order accurate vortex methods with explicit velocity kernels. J Comput Phys. 1985;58:188–208.

[13] Hald OH. Convergence of vortex methods for Euler's equations, III. SIAM J Numer Anal. 1987;24(3):538–582.

[14] Winckelmans GS, Leonard A. Contribution to Vortex Particle Methods for the Computation of Three-Dimensional Incompressible Unsteady Flows. J Comput Phys. 1993;109:247–273.

[15] Hejlesen MM, Rasmussen JT, Chatelai P, Walther JH. A high order solver for the unbounded Poisson equation. J Comput Phys. 2013;Under review.

[16] Abramowitz M, Stegun IA. Handbook of Mathematical Functions With Formulas, Graphs and Mathematical Tables. National Bureau of Standards. Applied Mathematics Series. 55; 1972.

[17] Raviart PA. Particle approximation of first order systems. J Comput Math. 1986;4(1):50–61.

[18] Hald OH. Convergence of vortex methods for Euler's equations. II. SIAM J Numer Anal. 1979;16:726–755. 5.

[19] Beale JT, Majda A. Vortex methods. I: Convergence in Three Dimensions. Math Comput. 1982;39(159):1–27.

[20] Beale JT, Majda A. Vortex Methods. II: Higher Order Accuracy in Two and Three Dimensions. Math Comput. 1982;39(159):29–52.

[21] Cottet GH, Koumoutsakos P. Vortex Methods – Theory and Practice. New York: Cambridge University Press; 2000.